Journal of Research in Clinical Medicine

J Res Clin Med. 2025;13:33323
doi: 10.34172/jrcm.025.33323
https://jrcm.tbzmed.ac.ir

TUOMS PRESS

Original Article

Brain tumour detection in MRI images using elastic net regression

Srinivasarao Gajula[1,2*], **V. Rajesh**[1]

[1]Departments of ECE, Koneru Lakshmaiah Educational Foundation, Guntur, India
[2]Departments of ECE, St.Ann's College of Engineering & Technology, Chirala, India

Article info

Article History:
Received: July 25, 2022
Revised: October 25, 2024
Accepted: October 29, 2024
ePublished: December 13, 2025

Keywords:
Elastic nets, MRI scan, Threshold limit values

Abstract

Introduction: Magnetic resonance imaging (MRI) scans of the brain are used to identify signs of disease, enabling more precise diagnosis of brain-related conditions. Neurological disorders pose significant risks and can lead to the deterioration of normal bodily functions. Various strategies are employed to monitor anomalies. However, significant improvements are still required in diagnostic processes and in the detection of cerebral diseases.

Methods: This method first involved preprocessing the image, followed by threshold-based segmentation. We used elastic net regression (ENR) due to its superior performance metrics compared to the approaches we evaluated for image classification.

Results: This strategy yielded improved outcomes, with an accuracy of 98.7% and precision of 98.88%. The recall score was 98.75%, while the F1 score was 98.23%.

Conclusion: In this study, the TSENR method was used to detect brain disease. Although many techniques are used to diagnose neurological disorders, not all of them are suitable for reliable evaluation. However, the implemented TSENR model provided a more accurate, sensitive, and predictive response. This technique can be applied to medical image analysis.

Introduction

Major neurological disorders include Alzheimer's disease (AD), transient ischemic attack (TIA), and brain tumours. These conditions affect populations worldwide. There are various types of brain disorders. Joint regression and classification in a sparse multi-task learning framework are used to develop a novel feature selection method for AD diagnosis. The method uses observational relational information feature-feature, response-response, and sample-sample—to increase feature-sample similarity. We create an objective function with these relationships and an ℓ2,1-norm regularization term, optimized with an efficient approach. Based on ADNI dataset experiments, our strategy outperforms ADAS-Cog and MMSE in clinical score prediction and disease state diagnosis.[1] A Bayesian random effects model with credible intervals comprising 95% of the total was utilized. This heterogeneity was assessed using the I^2 statistic.[2] Fluid biomarkers and neuroimaging techniques are used to identify tumours.[3] Based on existing data, machine learning can efficiently categorize different tumour types.[4] The initial cognitive and behavioural symptoms experienced by patients with AD vary greatly. The prevalence of these symptoms varies with age; younger patients more often present with non-memory cognitive and behavioural symptoms.[5] There is particular emphasis on the national policies for managing AD, anticipated challenges due to shortage in social care staff, and future budgetary requirements of the state.[6] AD has a preclinical phase that begins years prior to dementia diagnosis, representing a critical opportunity for intervention. The National Institute on Aging and the Alzheimer's Association convened an international workgroup to evaluate various evidence types and provide recommendations for predicting the risk of transitioning from "normal" cognition to mild cognitive impairment (MCI) and AD dementia. A conceptual framework and operational criteria for research are proposed to standardize preclinical AD studies and facilitate early intervention when treatments may be most effective, noting that these recommendations are intended for research purposes only and hold no clinical implications.[7] A deep learning strategy was proposed for shared latent feature representation from magnetic resonance imaging (MRI) and PET using a deep belief model (DBM). This method systematically finds a joint feature representation from multiple modalities, differing from earlier approaches that fused Gray Matter (GM) tissue densities and voxel intensities. The proposed technique leverages deep learning for self-teaching high-level features to efficiently integrate information from MRI

***Corresponding Author:** Srinivasarao Gajula, Email: gsrinivasarao443@gmail.com

and positron emission tomography (PET). Experiments on the ADNI dataset indicate that this strategy surpasses previous methods in quantitative metrics.[8] Low-level features can contain complex patterns, including non-linear interactions. By combining latent information with low-level features, it is possible to build a strong model for AD/MCI classification with high diagnostic accuracy.[9] ADNI examined MCI patients' MRI and Cerebrospinal Fluid (CSF) biomarkers to predict AD conversion. Non-converters had worse Spatial Pattern of Abnormality for Recognition of Early Alzheimer's Disease (SPARE-AD) scores and brain atrophy than converters. Midlevel SPARE-AD suggested rapid atrophy, while negative MCI-NC had higher MMSE scores and slower declines. Even though baseline evaluations were sensitive, many MCI-NC had aberrant outcomes that warranted more study. CSF biomarkers and SPARE-AD enhanced prediction.[10] Simultaneous spatio-spectral filter optimization estimates the posterior probability density function that distinguishes single-trial EEG signals associated with specific mental activity. The posterior probability density function was estimated using a particle-based approximation method that combines factored sampling with a diffusion process.[11] Support vector machine (SVM) and high-dimensional classification techniques are used to detect AD and moderate cognitive impairment from MRI data. The paper introduces a local patch-based subspace ensemble method that employs multiple local classifiers to enhance accuracy and resilience, addressing the challenges posed by noisy neuroimaging data. Through random sampling of brain image patches, a weak local spatial consistency classifier is generated. Tests conducted on 652 subjects from the ADNI database revealed that this method achieved 90.8% accuracy and 94.86% AUC for AD diagnosis, as well as 87.85% accuracy and 92.90% AUC for MCI, thereby outperforming existing classification methods.[12] To improve AD landmark detection, additional significant and reliable anatomical landmarks were identified. Morphological features and AD landmarks were used to develop an SVM classifier for AD prediction.[13] A data-driven learning approach was used to identify tumours disease-related anatomical landmarks in brain MR scans and surrounding image patches.[14] Multiple kernels are integrated into a unified approach to classify AD. This objective is achieved by incorporating the attributes of nodes and edges into the network, which encompass high accuracy, throughput, and recall. However, necessary changes are required.[15] In nearly 80% of cases, complex sustained attention, semantic memory, working memory, episodic memory, and selective attention identified outcomes accurately, according to a discriminant function analysis. The false positive rate was 5.93%, substantially lower than prior MCI investigations. The findings imply that sensitive and targeted neuropsychological tests can greatly reduce MCI false positives.[16]

Among our numerous achievements, we have successfully delineated the roadmap technique, which is based on the biomark model.[17] The information that was shown earlier indicates that various models are capable of simultaneously achieving impressive levels of accuracy, throughput, and recall. Nevertheless, more changes are necessary.[18] AD profoundly affects the hippocampus. A novel, fully automated technique for hippocampus segmentation employing probabilistic and anatomical priors has been established to address the constraints of manual segmentation.[19] A hippocampal-focused MRI classification method for AD is suggested. A late fusion technique blends hippocampus feature and CSF volume classification data. This combination strategy distinguishes AD from MCI better than volumetric methods in experiments. Future study may include numerous ROIs and MRI modalities in the categorization system.[20] The study introduces a new method for automatically identifying segmented brain MRIs from ADNI participants using independent component analysis (ICA) and supervised learning. Normalizing and segmenting MRI with SPM8, generating average images for normal, MCI, and AD individuals, and extracting independent components with fast ICA are the three processes. Each brain image is projected onto this space for feature extraction and classification with an SVM.[21] A kernel-based method utilizing mean cortical thickness was employed to network the 83 participants of the Open Access Series of Imaging Studies, comprising both normal controls (NC) and AD patients. Machine learning techniques were developed to utilize edge characteristics of networks to predict AD/NC. This hybrid feature selection method combines filter and wrapper techniques to mitigate the difficulties posed by high-dimensional data, characterized by an abundance of features compared to samples, hence facilitating the training of SVMs with the selected features.[22] Brain abnormalities are automatically detected using logistic regression machine learning on MRI brain pictures. Many obsolete tumor detection technologies are ineffective. Machine intelligence is needed to correct these issues. Real-time MRI scans are tested across orientations and age groups for illness categorization using logistic regression and threshold segmentation.[23]

The main objective of the paper is to use threshold segmentation along with the ENR machine learning method; we aimed to detect tumor-related abnormalities. And to identify tumors in brain MRI images and to enable fast and accurate diagnosis of different tumor types.

Proposed work

In this study we used threshold segmentation and elastic net regression (ENR) for disease identification. MRI data sets were collected from ADNI-1, ADNI-2 and Minimal Interval Resonance Imaging in Alzheimer's Disease (MIRIAD). In the first stage, preprocessing was

performed on MRI images using histogram equalization and segmentation. In the next step, after preprocessing, a segmentation mechanism was applied to the processed image. Global thresholding was used as the first step because it can switch between simple and complex patterns recognition. To determine abnormal regions in the image, we used global threshold-based segmentation.

Global threshold segmentation

In this process, we first selected the MRI brain image. In the second step, we calculated the threshold value, which produced two groups of pixel values. Using these two groups, we calculated their mean values. A new threshold value was calculated as the average of those two mean values. this process was repeated until convergence across consecutive iterations.

As shown in Figure 1, the initial stage involves used a B1-weighted MRI brain image as input to preprocessing, and the output of it subsequently was fed into the segmentation process. The segmented image was then provided as input to the classifier.

Feature extraction and classification

Different features of MRI images were extracted using the ENR mechanism. Several regression mechanisms can be used for classification, but only a few are effective in this context. ENR-based logistic regression mechanisms can be used to determine disorders in medical image applications.

In this context, γ denotes the patient's problem-solving abilities and attention characteristics. This element is associated with reduced access time and increased frequency. The β component reflects the patient's brain activity and the functionality of distinct regions. This, facilitates the effective analysis of patients' metastatic conditions; moreover, α and θ images correspond to the patient's MRI brain scans, respectively. The Δ component indicates the presence of brain disease.

$$\Psi(t) = cos(5t)\,exp(-t^2/2) \tag{1}$$

$$h_j(out) = \Psi_{a,c}(j) = cos\left(5 * \frac{\sum_{k=1}^{m} W_{jk} x_k - c_j}{a_j}\right) * exp\left(-\frac{1}{2}\left(\frac{\sum_{k=1}^{m} W_{jk} x_k - c_j}{a_j}\right)^2\right) \tag{2}$$

Figure 2 explains the flow of ENR, where β serves as the initial parameter for aggregating the values with weights for classification. Equations (1) and (2) were used to determine the output of the wavelet autoencoder based on a sigmoid function . The result is a econstructed model derived from an autoencoder.

$$E = \frac{1}{s}\sum_{s=1}^{s}\left[\frac{1}{2}\sum_{i=1}^{m}\left(\hat{x}_i^s - x_i^s\right)^2\right] + \beta\left(\sum_{j=1}^{p} p\log\frac{p}{\hat{p}_j} + (1-p)\log\frac{1-p}{1-\hat{p}_j}\right) \tag{3}$$

The multidimensional input image and the output that was reconstructed are both represented by equation 3, which is part of the equation. $\hat{x}_i^s$ & x_i^s is the representation of the image that was entered. $p\log\frac{p}{\hat{p}_j}$ is the function of divergence that was shown by it. These parameters were required to reconstruct the output image.

$$W_{ij}(t+1) = W_{ij}(t) - \eta\frac{\partial E(t)}{\partial W_{ij}} + \alpha\Delta W_{ij}(t) \tag{4}$$

$$W_{ij}(t+1) = W_{ij}(t) - \eta\frac{\partial E(t)}{\partial W_{ij}} + \alpha\Delta W_{ij}(\mathrm{t}) \tag{5}$$

$$\alpha(t+1) = a_j(t) - \eta\frac{\partial E(t)}{\partial \alpha_j} + \alpha\Delta a_j(\mathrm{t}) \tag{6}$$

$$c_j(t+1) = c_j(t) - \eta\frac{\partial E(t)}{\partial c_j} + \alpha\Delta c_j(\mathrm{t}) \tag{7}$$

Equations (4) to (7) define the optimal training parameters, which we used to minimize the error during reconstruction. The sole method to achieve these goals is via threshold iterations; hence, to improve the efficacy of the super learning features, we must construct the stack architecture.

$$H\beta = T$$

$$\mathrm{H} = \begin{bmatrix} g(w_1.X_1 + b_1) & \cdots & g(w_s.X_1 + b_s) \\ \vdots & \cdots & \vdots \\ g(w_1.X_s + b_1) & \cdots & g(w_s.X_s + b_s) \end{bmatrix}_{s*s} \tag{8}$$

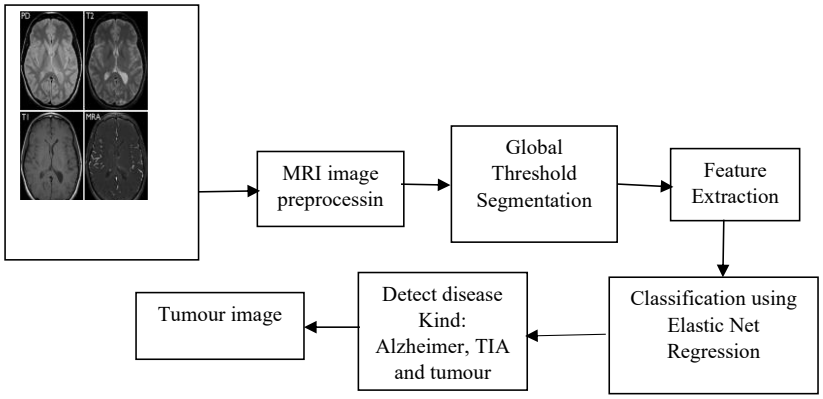

Figure 1. Block diagram of TSENR

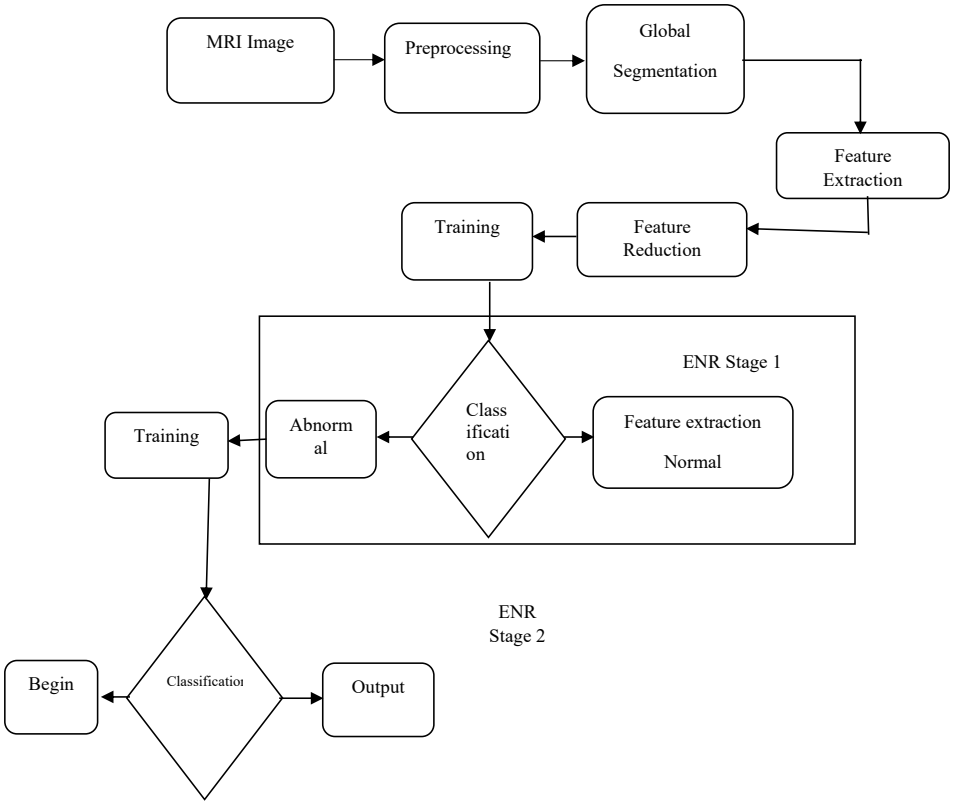

Figure 2. Elastic net regression

$$\beta = \begin{bmatrix} \beta_1 \\ \vdots \\ \beta_{sizem} \end{bmatrix} \text{ and } T = \begin{bmatrix} t_1 \\ \vdots \\ t_{sizem} \end{bmatrix} \quad (9)$$

Equations (8) and (9) describe the confused matrix, which provides a means to extract latent information. H denotes the output matrix, β denotes the output weighted vector, and T denotes the target matrix. We used these mathematical steps to obtain the matrix that best represents the brain.

Classification using elastic net regression

Various machine learning models are available for multidisciplinary applications; however, this type of medical image processing requires a more advanced algorithm. This objective was addressed using ENR. A key role of ENR is to evaluate both testing and training data, which is its fundamental feature. This helps reduce overfitting of the learning model. Oridinary least squares (OLS) models are commonly employed to calculate imaging errors. In this case, the cost and the error function were not computed using basic least squares equations, and direct error minimisation was not required.

$$\sum_{i=1}^{M}\left(y_i - \square_i\right)^2 = \sum_{i=1}^{M}\left(y_i - \sum_{j=0}^{p} w_j * w_{ij}\right)^2 \quad (10)$$

Equation (10) is used to calculate the predictive factors such asp1, p2, and p3 (for instance, height, gender, and diet). In this situation, p1 and p2 are correlated. However, the statistical parameter linked to p1 and p2 was not fulfilled by p3, as demonstrated by the previously presented equation.

$$\frac{\sum_{i=1}^{M}\left(y_i - x_i^j\hat{\beta}\right)^2}{2n} + \lambda\left(\frac{1-\alpha}{2}\sum_{j=1}^{m}\hat{\beta}_j^2 + \alpha\sum_{j=1}^{m}\left|\hat{\beta}_j\right|\right) \quad (11)$$

Equation (11) describes the ENR formulation, providing accurate outcomes through regularised estimation. The regularization property of LASSO is represented by L1, whereas the regularization of RIDGE is represented by L2. This model is effective for estimation while reducing both bias and variance. The L2 term penalises the magnitude of the coefficients, consistent with ridge regression. When λ equals zero, this equation becomes normalized. Consequently, diminishing coefficients lead to a reduction in variance, ultimately equating to zero. Therefore, we have used ENR instead of equations (10) and (11) to assess the coefficients, as shown in equation (12) below.

$$\hat{\beta} = arg_{\beta} minRSS\,(\hat{\beta}) = arg_{\beta} min\sum_{i=1}^{n}\left(y_i - \beta_0 - \sum_{j=1}^{k} x_{ij}\beta_j\right)^2 \quad (12)$$

$$\hat{\beta}_{Ridge} = arg_{\beta} minRSS\,(\beta) \quad (13)$$

$$= arg_{\beta} min\left\{\sum_{i=1}^{n}\left(y_i - \beta_0 - \sum_{j=1}^{k} x_{ij}\beta_j\right)^2 + \lambda\sum_{j=1}^{k}\beta_j^2\right\} \quad (14)$$

$$\hat{\beta}_{\text{LASSO}} = arg_{\beta} min\left\{\sum_{i=1}^{n}\left(y_i - \beta_0 - \sum_{j=1}^{k} x_{ij}\beta_j\right)^2 + \lambda\sum_{j=1}^{k}\left|\beta_j\right|\right\} \quad (15)$$

$$R_{adj}^2 = 1\text{-}\left(1-R^2\right)\frac{n-1}{n-p-1} \quad (16)$$

The computation of the ENR fit is defined in equations (12-16). In these equations, the R_{adj}^2 represents the coefficients of determination, the n signifies the sample size, and the letter p specifies the entire number of parameters in the model.

$$X = TP^T + E$$

$$Y = TQ^T + F$$

$$T = XW\left(P^TW\right)^{-1} \quad (17)$$

T, P, and E represent the score, loading, and residual of X, respectively. The following variables are employed in the computation of the partial least square errors. No machine learning algorithm exists that accommodates this specific choice.

$$\hat{y} = X_{new}\beta_{PLS}$$

$$\beta_{PLS} = W\left(P^TW\right)^{-1}Q^T \quad (18)$$

Equation (18) illustrates the k-fold validation function, which provides the principal component values in the ENR. We used the above steps for the classification of MRI images in seizure diagnosis.

After these operations, we calculated the error rate, accuracy, F1 score, and true positive rate. In this work, we applied the threshold-based preprocessing and then performed classification using ENR. The mathematical formulations above were used to compute these performance metrics.

1. $RMSEP = \sqrt{\frac{\sum_{i=1}^{n}\left(y_i - \hat{y}_i\right)^2}{n}}$

$$\frac{RMSEP\left(i^*\right)}{RMSEP\left(i\right)} \geq \lambda \quad (19)$$

2. $NMSE = \frac{\sum_{i=1}^{n}(y_i - \hat{y}_i)^2}{y_i^2}$ (20)

3. $\hat{\beta}_{enet} = \left(1+\frac{\lambda_2}{n}\right)\left\{arg_{\beta}\min\lambda - \sum_{j=1}^{p} x_i\beta_j{}^2 + \lambda_1\beta_1 + \lambda_1\beta_2{}^2\right\}$ (21)

4. Accuracy = $\hat{\beta}_{enet} + R_{adj}^2 / = \hat{\beta}_{enet} + R_{adj}^2 + \text{F}_\text{p} + \text{F}_\text{n}$. (22)

5. F_l score = $\text{F}_\text{p} + \text{F}_\text{n}./\text{T}_\text{p}$. (23)

6. $\text{T}_\text{p} = 1\text{-}\frac{SSR}{SST}$. (24)

These mathematical equations were the primary tools for assessing the efficiency of the proposed threshold-ENR approach. In this context, sensitivity refers to the true positive rate, whereas accuracy reflects the overall correctness of classification outcomes. Specificity refers to the ratio of the true negative rate.

Dataset

In this work, we used datasets such as ADNI-1, ADNI-2 and MIRIAD for classification purpose. These three datasets were also used for future extractions.

Performance metrics

The following equations were used to determine the throughput, accuracy and recall.

$$\text{AC} = \frac{\text{TP}+\text{TN}}{\text{TP}+\text{TN}+\text{FP}+\text{FN}} \quad (25)$$

$$\text{R} = \frac{\text{TP}}{\text{TP}+\text{FN}} \quad (26)$$

Methods

This study utilized the TSENR method to identify brain-affecting diseases. Conversely, the TSENR model yielded a more accurate, sensitive, and predictive response. It can be used for medical image analysis.

Results

By using global thresholding we extracted the features of brain images and for classification purpose we used ENR. Figure 3 demonstrates that a B1-weighted image was utilized as the input and that it underwent preprocessing using various specific methods. Figure 4a illustrates the "Global Thresholding image," which is a binary representation derived from a singular threshold value applied to the grayscale brain MRI. Pixels beyond the threshold are white, indicating possibly abnormal or high-intensity tissues such as cancers, whereas pixels below the threshold are black, denoting the background

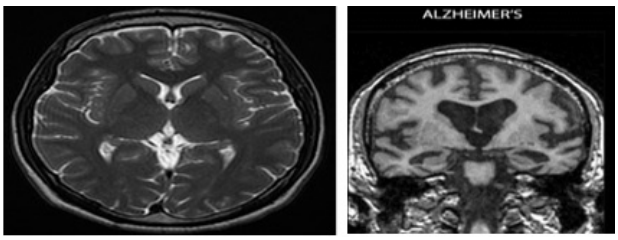

Figure 3. (a) B1 weighted image, (b) B2 weighted image

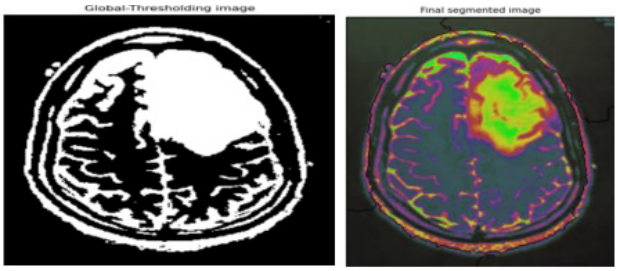

Figure 4. (a) Global thresholding image, (b) Segmented image

Table 1. Classification results for brain disorders on the ADNI dataset.

ADN12	Accuracy score (%)	Precision score (%)	Recall score (%)	F1 score (%)
Chupin[19]	85	74	83	78
Ben Ahmed[20]	87	75	78	70.7
Suk[8]	80.92	82.61	88.49	88.94
Khedher[21]	90.4	92.3	88.6	96.1
Dai[22]	90.18	91.54	90.61	91.08
Liu[15]	97.8	98.67	97.2	98.0
Proposed	98.7	98.88	98.75	98.23

or less significant tissues. This straightforward method distinguishes regions based on luminosity, yet fails to identify more intricate details. Figure 4b, "Final segmented image," displays the brain with color-coded regions. This image delineates the tumor or region of concern from the brain and provides anatomical context. Following thresholding, segmentation may encompass region growth, morphological techniques, or alternative clustering methods to delineate and display anomalous areas such as brain tumors.

Table 1 presents classification results for brain disorders derived from studies utilizing the ADNI dataset. The results encompass essential performance indicators for various models or methodologies, especially accuracy, precision, recall, and F1 score all represented as percentages.

Discussion

The study shows that medical imaging can diagnose brain-affecting neurological disorders using TSENR. TSENR had superior precision, sensitivity, and prediction accuracy compared to conventional approaches, making it acceptable for clinical evaluation. Traditional methods suffer from noise and anatomical variability, whereas TSENR is sophisticated architecture that better solves these issues.The TSENR model can extract discriminative patterns from complicated brain regions, improving neurological abnormality classification. Medical image analysis requires robustness, especially with different scanners and patient situations. The findings indicate that TSENR can be included in comprehensive diagnostic processes, enhancing current radiological assessments and offering measurable, consistent metrics to aid clinical decision-making. The sensitivity of TSENR to early structural alterations should greatly improve prompt diagnosis, as neurological illnesses frequently necessitate early intervention for optimal outcomes. The present work supports TSENR as an effective technique for medical image analysis, providing dependable identification of brain-related diseases. Ongoing improvement and validation will clarify its function in aiding physicians and enhancing diagnostic processes for neurological disease diagnosis.

Study Highlights

What is current knowledge?

Elastic net regression (ENR) effectively detects brain tumors in MRI images by selecting relevant imaging features from complex radiomic data. It aids in distinguishing tumor tissue from non-neoplastic tissue and enhances prediction and diagnosis through refined feature sets for machine learning classification. Its primary use lies in radiomics-based pipelines, contributing to feature reduction and model interpretability.

What is new here?

This method combines quick threshold-based segmentation with an ENR classifier instead of just using large deep networks, making it easier to understand and faster for detecting brain tumors in MRI scans and classifying tumor types. This makes your method a cost-effective option that keeps accuracy while improving clarity and ease of use in situations with limited computing power or data.

Limitation of the study

Elastic net can be computationally costly on large datasets due to the need for repeated model updating. The selection of tuning parameters can be challenging, as there is no single definite way to choose them. Although regression models can handle basic correlations between predictors and outcomes, they rely on assumptions that are often violated in real-world settings. Additionally, standard regression models typically handle only relatively simple correlations.

Conclusion

In the current study, we used the TSENR approach to identify brain-affecting disorders. Although many methods are available for diagnosing neurological disorders, not all of them are suitable for reliable evaluation. In contrast, the implementation of the TSENR model provided a more precise, sensitive, and predictive response. This method can be applied in medical image analysis.

Acknowledgments

The authors would like to thank the Koneru Lakshmaiah Educational Foundation, Guntur for their support.

Authors' Contribution

Conceptualization: Srinivasarao Gajula, V. Rajesh.
Data curation: Srinivasarao Gajula, V. Rajesh.
Formal analysis: Srinivasarao Gajula, V. Rajesh.
Funding acquisition: Srinivasarao Gajula, V. Rajesh.
Investigation: Srinivasarao Gajula, V. Rajesh.
Methodology: Srinivasarao Gajula, V. Rajesh.
Project administration: Srinivasarao Gajula, V. Rajesh.
Resources: Srinivasarao Gajula, V. Rajesh.
Software: Srinivasarao Gajula.

Supervision: V. Rajesh.
Validation: Srinivasarao Gajula, V. Rajesh.
Visualization: Srinivasarao Gajula, V. Rajesh.
Writing–original draft: Srinivasarao Gajula, V. Rajesh.
Writing–review & editing: Srinivasarao Gajula, V. Rajesh.

Competing Interests
None to declare.

Ethical Approval
Not applicable.

Funding
This study was self-funded.

References

1. Zhu X, Suk HI, Wang L, Lee SW, Shen D. A novel relational regularization feature selection method for joint regression and classification in AD diagnosis. Med Image Anal. 2017;38:205-14. doi: 10.1016/j.media.2015.10.008
2. Niu H, Álvarez-Álvarez I, Guillén-Grima F, Aguinaga-Ontoso I. Prevalence and incidence of Alzheimer's disease in Europe: a meta-analysis. Neurologia. 2017;32(8):523-32. doi: 10.1016/j.nrl.2016.02.016
3. Alzheimer's Disease International (ADI). World Alzheimer Report 2018 - The State of the Art of Dementia Research: New Frontiers. London, UK: ADI; 2018.
4. Perrin RJ, Fagan AM, Holtzman DM. Multimodal techniques for diagnosis and prognosis of Alzheimer's disease. Nature. 2009;461(7266):916-22. doi: 10.1038/nature08538
5. Barnes J, Dickerson BC, Frost C, Jiskoot LC, Wolk D, van der Flier WM. Alzheimer's disease first symptoms are age dependent: evidence from the NACC dataset. Alzheimers Dement. 2015;11(11):1349-57. doi: 10.1016/j.jalz.2014.12.007
6. Marešová P, Mohelská H, Dolejš J, Kuča K. Socio-economic aspects of Alzheimer's disease. Curr Alzheimer Res. 2015;12(9):903-11. doi: 10.2174/1567205012091510191114 48
7. Sperling RA, Aisen PS, Beckett LA, Bennett DA, Craft S, Fagan AM, et al. Toward defining the preclinical stages of Alzheimer's disease: recommendations from the National Institute on Aging-Alzheimer's Association workgroups on diagnostic guidelines for Alzheimer's disease. Alzheimers Dement. 2011;7(3):280-92. doi: 10.1016/j.jalz.2011.03.003
8. Suk HI, Lee SW, Shen D. Hierarchical feature representation and multimodal fusion with deep learning for AD/MCI diagnosis. Neuroimage. 2014;101:569-82. doi: 10.1016/j.neuroimage.2014.06.077
9. Suk HI, Shen D. Deep learning-based feature representation for AD/MCI classification. Med Image Comput Comput Assist Interv. 2013;16(Pt 2):583-90. doi: 10.1007/978-3-642-40763-5_72
10. Davatzikos C, Bhatt P, Shaw LM, Batmanghelich KN, Trojanowski JQ. Prediction of MCI to AD conversion, via MRI, CSF biomarkers, and pattern classification. Neurobiol Aging. 2011;32(12):2322.e19-27. doi: 10.1016/j.neurobiolaging.2010.05.023
11. Suk HI, Lee SW. A novel Bayesian framework for discriminative feature extraction in brain-computer interfaces. IEEE Trans Pattern Anal Mach Intell. 2013;35(2):286-99. doi: 10.1109/tpami.2012.69
12. Liu M, Zhang D, Shen D. Ensemble sparse classification of Alzheimer's disease. Neuroimage. 2012;60(2):1106-16. doi: 10.1016/j.neuroimage.2012.01.055
13. Zhang J, Gao Y, Gao Y, Munsell BC, Shen D. Detecting anatomical landmarks for fast Alzheimer's disease diagnosis. IEEE Trans Med Imaging. 2016;35(12):2524-33. doi: 10.1109/tmi.2016.2582386
14. Liu M, Zhang J, Adeli E, Shen D. Landmark-based deep multi-instance learning for brain disease diagnosis. Med Image Anal. 2018;43:157-68. doi: 10.1016/j.media.2017.10.005
15. Liu J, Wang J, Hu B, Wu FX, Pan Y. Alzheimer's disease classification based on individual hierarchical networks constructed with 3-D texture features. IEEE Trans Nanobioscience. 2017;16(6):428-37. doi: 10.1109/tnb.2017.2707139
16. Klekociuk SZ, Summers JJ, Vickers JC, Summers MJ. Reducing false positive diagnoses in mild cognitive impairment: the importance of comprehensive neuropsychological assessment. Eur J Neurol. 2014;21(10):1330-6. doi: 10.1111/ene.12488
17. Weissberger GH, Strong JV, Stefanidis KB, Summers MJ, Bondi MW, Stricker NH. Diagnostic accuracy of memory measures in Alzheimer's dementia and mild cognitive impairment: a systematic review and meta-analysis. Neuropsychol Rev. 2017;27(4):354-88. doi: 10.1007/s11065-017-9360-6
18. Frisoni GB, Boccardi M, Barkhof F, Blennow K, Cappa S, Chiotis K, et al. Strategic roadmap for an early diagnosis of Alzheimer's disease based on biomarkers. Lancet Neurol. 2017;16(8):661-76. doi: 10.1016/s1474-4422(17)30159-x
19. Chupin M, Gérardin E, Cuingnet R, Boutet C, Lemieux L, Lehéricy S, et al. Fully automatic hippocampus segmentation and classification in Alzheimer's disease and mild cognitive impairment applied on data from ADNI. Hippocampus. 2009;19(6):579-87. doi: 10.1002/hipo.20626
20. Ben Ahmed O, Benois-Pineau J, Allard M, Ben Amar C, Catheline G. Classification of Alzheimer's disease subjects from MRI using hippocampal visual features. Multimed Tools Appl. 2015;74(4):1249-66. doi: 10.1007/s11042-014-2123-y
21. Khedher L, Ramírez J, Górriz JM, Brahim A, Illán IA. Independent component analysis-based classification of Alzheimer's disease from segmented MRI data. In: International Work-Conference on the Interplay Between Natural and Artificial Computation. Cham: Springer International Publishing; 2015. p. 78-87. doi: 10.1007/978-3-319-18914-7_9
22. Dai D, He H, Vogelstein JT, Hou Z. Accurate prediction of AD patients using cortical thickness networks. Mach Vis Appl. 2013;24(7):1445-57. doi: 10.1007/s00138-012-0462-0
23. Gajula S, Rajesh V. An MRI brain tumour detection using logistic regression-based machine learning model. Int J Syst Assur Eng Manag. 2024;15(1):124-34. doi: 10.1007/s13198-022-01680-8